Enzyme and Microbial Technology 44 (2009) 170–175

Contents lists available at ScienceDirect

Enzyme and Microbial Technology

journal homepage: www.elsevier.com/locate/emt

Designing the substrate specificity of D-hydantoinase using a rational approach

Sang-Chul Lee[a,1], YoungJung Chang[b,1], Dong-Min Shin[a], Jieun Han[a], Moon-Hyeong Seo[a], Hossein Fazelinia[b], Costas D. Maranas[b], Hak-Sung Kim[a,*]

[a] Department of Biological Sciences, Korea Advanced Institute of Science and Technology, 373-1, Gusung-dong, Yusung-gu, Daejeon 305-701, Republic of Korea
[b] Department of Chemical Engineering, The Pennsylvania State University, University Park, PA 16802, USA

ARTICLE INFO

Article history:
Received 20 August 2008
Received in revised form 23 October 2008
Accepted 24 October 2008

Keywords:
Rational design
D-Hydantoinase
Non-natural D-amino acid
Substrate specificity
Hydroxyphenylhydantoin

ABSTRACT

Enzymes that exhibit superior catalytic activity, stability and substrate specificity are highly desirable for industrial applications. These goals prompted the designed substrate specificity of *Bacillus stearothermophilus* D-hydantoinase toward the target substrate hydroxyphenylhydantoin (HPH). Positions crucial to substrate specificity were selected using structural and mechanistic information on the structural loops at the active site. The size and hydrophobicity of the involved amino acids were rationally changed, and the substrate specificities of the designed D-Hyd mutants were investigated. As a result, M63I/F159S exhibited about 200-fold higher specificity for HPH than the wild-type enzyme. Systematic mutational analysis and computational modeling also supported the rationale used in the design.

1. Introduction

The exquisite substrate specificity and high catalytic efficiency of a variety of enzymes have been exploited in chemical synthesis, synthetic biology, and medicine. Despite this success, many enzymes are still unfavorable for such practical purposes due to their limitations in substrate specificity, turnover rate, stability, and expression level. To address this issue, many advances have been made with methods including a structure-based rational design and directed evolution [1–3]. Recently, computational approaches have proved to be effective for the design of enzymes with new functions [4]. As an alternative to a rational design approach, a combinatorial active site saturation test (CAST) was proposed [5]. This method was reported to enable a systematic search of relatively small focused library around the active site of an enzyme, accelerating the identification of desired enzyme mutations.

Microbial hydantoinase (Hyd) is used in conjunction with *N*-carbamoylase for the commercial production of optically pure D- and L-amino acids that are intermediates for the synthesis of semi-synthetic antibiotics, peptide hormones, pyrethroids, and pesticides [6,7]. Hyd catalyzes the hydrolysis of the cyclic amide bond of 5′-monosubstituted hydantoins (Fig. 1). We previously cloned and overexpressed D-hydantoinase (D-Hyd) from *Bacillus stearothermophilus* SD1, and demonstrated the enzymes' strict enantioselectivity, high catalytic activity, ease of overexpression, and thermostability [8]. Despite these distinct advantages, the substrate specificity of D-Hyd is biased toward non-substituted hydantoin, which is undesirable for the synthesis of commercially important unnatural amino acids with aromatic side chains such as phenyl and hydroxyphenyl groups (Fig. 1). For example, D-4-hydroxyphenylglycine (D-HPG), which is commercially produced from hydroxyphenylhydantoin (HPH) via sequential reactions of D-Hyd and *N*-carbamoylase, is used as the intermediate for semi-synthetic antibiotics such as amoxycillin and cefadroxil [9].

Appropriately, attempts to engineer hydantoinases and the reaction condition have been undertaken. There were reports regarding optimization of whole-cell reaction condition for the production of D-HPG and construction of hydantoinase–carbamoylase fusion protein system [10,11]. In a series of studies, D-Hyd was re-engineered using random mutagenesis, saturation mutagenesis, and screening to invert enantioselectivity, converting D-selective hydantoinase to an L-selective enzyme, and increased total enzyme activity [12]. In another study based on a rational approach to engineer substrate specificity of Hyd with structural analysis, the substrate and corresponding binding amino acid were exploited to create a variant of Hyd with higher substrate specificity toward the large substituent group [13]. Other approaches included improving thermostability of Hyd by truncation and fusion of the enzyme from difference sources [14] and use of C-terminal truncation and substitution to generate monomeric Hyd from the original dimeric structure without affecting the activity [15].

* Corresponding author. Tel.: +82 42 350 2616; fax: +82 42 350 2610.
E-mail address: hskim76@kaist.ac.kr (H.-S. Kim).
[1] These authors equally contributed to this work.

0141-0229/$ – see front matter © 2008 Elsevier Inc. All rights reserved.
doi:10.1016/j.enzmictec.2008.10.020

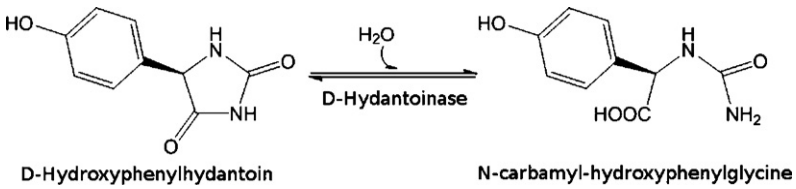

Fig. 1. Reaction of hydantoinase. Hydrolysis of D-HPH by D-hydantoinase.

Here, we report the redesign of Hyd to have high specificity toward substrates with aromatic side chains using a rational approach with structural consideration. Hydroxyphenylhydantoin was employed as the target substrate since it is the starting substrate for the production of D-HPG. The recently deduced crystal structure of D-Hyd has revealed a typical $(\beta/\alpha)_8$-barrel structure and three β/α-connecting loops (stereochemistry gate loops; SGLs) (Fig. 2a) as the major determinants of substrate specificity [16]. We first identified the critical residues on the structural loops at the active site of the D-Hyd and selected the design positions that could increase the specific activity toward the target substrate HPH compared to wild-type D-Hyd. Mutant enzymes were designed by optimizing the size and hydrophobicity of the selected amino acid residues, and the resulting enzymes were investigated in terms of kinetic constants. Efficacy of the design procedure was supported by systematic mutation analysis and computational modeling.

2. Materials and methods

2.1. Materials, bacterial strain, and vector

B. stearothermophilus SD1 was used as the source of the gene encoding D-Hyd. *Escherichia coli* JM109 was the host for the expression of wild-type and mutant enzymes. Plasmid pMAL-c2x used for the expression of fusion proteins was obtained from New England Biolabs (Beverly, MA) as were enzymes used for gene manipulation. Oligonucleotide synthesis was performed by Bioneer (Daejon, Korea). All other molecular biology reagents were purchased from commercial sources and were of analytical grade. HPH was purchased from Tokyo Chemical Industry (Tokyo, Japan). The high-pressure liquid chromatography (HPLC) column utilized for the activity assay was ODS-A from YMC (Kyoto, Japan).

2.2. Construction of mutants

Designed mutations were incorporated by an overlapping polymerase chain reaction (PCR) method using complementary oligonucleotides. Primer sequences are listed in Table 1. The mutant genes were incorporated into the pMAL-c2x vector in the restriction site between *Eco*RI and *Pst*I. *E. coli* JM109 cells were transformed by electroporation with the construct. Wild-type and mutant enzymes were purified as maltose binding protein-fused forms in the pMAL-c2x vector system. Expression of fusion proteins was achieved by addition of 0.2 mM isopropyl-β-D-thiogalactopyranoside (IPTG) at 37 °C when an optical density at 600 nm reached about 0.5. After cultivation for 3 h, the induced cells were harvested by centrifugation at 13,000 × *g* for 10 min and the pellets were resuspended in 20 mM Tris buffer (200 mM NaCl, 1 mM EDTA, pH 7.4). The suspended cells were disrupted by sonication and the supernatant was obtained after centrifugation at 13,000 × *g* for 15 min. The solution was purified using an amylose resin [17]. Proteins were analyzed by sodium dodecyl sulfate-polyacrylamide gel electrophoresis (SDS-PAGE), and proteins were quantified by using Bradford method [18]. The levels of wild-type and mutant Hyd in the soluble fraction were 0.5–1 mg protein per 5 ml culture medium.

2.3. Enzyme assay

The reaction mixture for the D-Hyd assay contained 1 mM $MnCl_2$, 10 mM D,L-HPH or 200 mM hydantoin, and 1–10 μg of enzyme in 0.1 ml of 0.1 M Tris–HCl buffer (pH 8.0). The enzyme reaction was carried out at 37 °C for 20 min. The amount of product was determined using HPLC [19] or colorimetrically using *p*-dimethylaminobenzaldehyde [20]. The HPLC elution solvent was 10% acetonitrile and the solvent flow rate was 0.5 ml/min. The eluted product was detected at 214 nm. For the spectrophotometric detection of the colored *p*-dimethylaminobenzaldehyde reagent, the absorbance was measured at 420 nm. The extinction coefficient of *N*-carbamylglycine was 174 L mol^{-1} cm^{-1}. One unit of activity was defined as the amount of enzyme required to produce 1 μmol of *N*-carbamyl-D-amino acid per min under the specified conditions. Activity of enzyme refers to the specific activity which is defined as the amount of product produced per min per mg protein. Activity was expressed as relative value to that of wild-type enzyme.

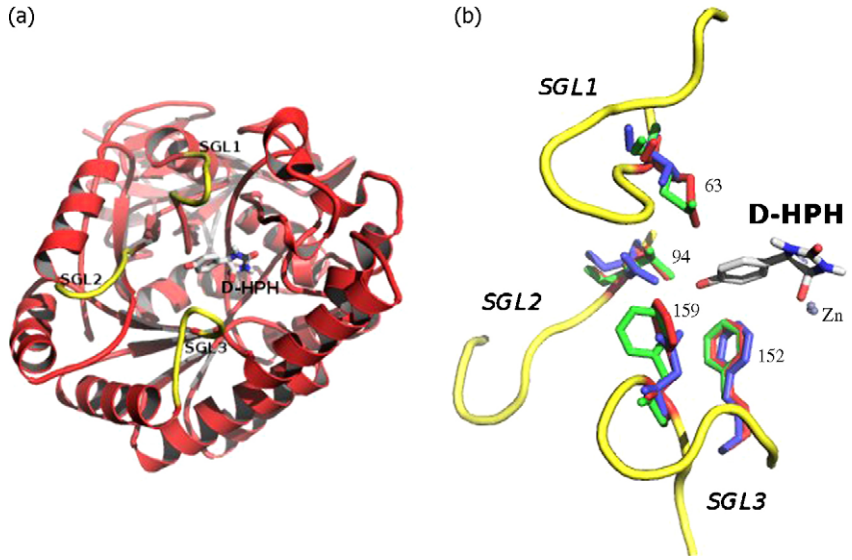

Fig. 2. Structure of D-hydantoinase. (a) Overall structure of D-hydantoinase and binding structure with D-hydroxyphenylhydantoin (D-HPH). (b) Coordination of amino acids at the binding site in three hydantoinases. Four residues are in 4 Å vicinity of hydroxide in HPH, which are M63, L94, F152, and F159 of Hyd (PDB ID: 1K1D, red). All the four amino acids reside on stereochemistry gate loops (SGLs, yellow). Amino acid residues of other hydantoinases at the same positions are compared (PDB ID: 1YNY, green; 1NFG, blue). The residues at 63rd and 159th positions are found to be significantly different from each other.

Table 1
List of primers used for site-directed mutagenesis.

Mutation position	Name	Sequence (5′ to 3′)[a]
M63	M63I	cacacgcatttagatATTccgcttggc
	M63A	cacacgcatttagatGCGccgcttggc
	M63H	cacacgcatttagatCATccgcttggc
	M63Q	cacacgcatttagatCAGccgcttggc
	rM63[b]	atctaaatgcgtgtgcggatc
F159	F159S	tttatggcgtataaaaacgtaTCCcaggcagatgat
	F159A	tttatggcgtataaaaacgtaGCGcaggcagatgat
	F159T	tttatggcgtataaaaacgtaACAcaggcagatgat
	F159N	tttatggcgtataaaaacgtaAACcaggcagatgat
	F159R	tttatggcgtataaaaacgtaCGCcaggcagatgat
	rF159[b]	tacgtttttatacgccataaa
Terminal[c]	5′-end	tagaattcatgacaaaaattataaaaaatg
	3′-end	tactgcagttaaatggttaattcctcgctc

Restriction sequences are shown with capital letter.
[a] Sequences of mutating nucleotides are shown with capital letter.
[b] Reverse primers were designed to be used generally with mutation of same position.
[c] 5′ end were tailed with *Eco*RI recognition sequence and 3′ end were tailed with *Pst*I sequence (underlined).

Kinetic constants of enzymes for hydantoin and HPH were determined from Lineweaver–Burk plot assuming Michaelis–Menten kinetics. Reaction conditions were set at 37 °C for 10 min. Highest concentrations of HPH and hydantoin were limited to 10 and 400 mM, respectively, due to their low solubilities. Thus, the concentration range of HPH and hydantoin was 1–10 and 50–400 mM, respectively.

2.4. Molecular modeling

The three-dimensional (3D) structure of the mutant enzymes was predicted by use of homology modeling with the wild-type structure (PDB ID: 1K1D) as the template [21]. For the loop refinement of the structure, DOPE potential was utilized [22]. Docking of D-HPH into the active site of each mutant enzyme was carried out using the CHARMm force field [23–25] and taking metal ions into account [26]. Binding pockets for the docking were pre-screened such that hydantoin ring of D-HPH was closely placed to the conserved catalytic residues of S288 and N337. Both ground and transition states of D-HPH were docked into the mutants for better representation of reaction mechanism [27]. For molecular visualization, the PyMOL molecular graphics and modeling package (http://www.pymol.org/) was used to generate the figure (http://www.povray.org/). GIMP software (http://www.gimp.org/) was used to edit and label figures when necessary.

3. Results and discussion

3.1. Selection of amino acid residues for design of substrate specificity

We investigated the protein sequence and 3D structure of homologous Hyds (PDB ID: 1K1D, 1YNY, 1NFG) based on mechanism and structure to select target residues. The design target was 1K1D cloned from *B. stearothermophilus* (BstHyd). Among the Hyds whose structures are currently known in PDB, 1YNY cloned from *Bacillus* sp. AR9 (designated BspHyd) [28] is most similar to BstHyd. These enzymes display 75% sequence identity and a structure root mean square deviation (RMSD) of 0.6 Å. The 1NFG cloned from *Burkholderia pickettii* (designated BpiHyd) [29] is less similar to 1K1D, displaying only 52% sequence identity and a RMSD of 1.1 Å. However, 1NFG has substrate preference toward the hydrophilic substituent hydantoin and the substrate target HPH is also a hydrophilic substituent hydantoin.

We focused on amino acid residues near the hydroxyphenyl group of docked D-HPH in the binding pocket to identify critical amino acid residues. Seven amino acids that lay within 4 Å of the pocket were selected for the design candidate pool, which included H60, M63, L94, carboxylated K150 (Kcx150), F152, Y155, and F159. These residues were compared among homologous hydantoinases, and their reaction mechanisms were analyzed (Table 2 and Fig. 2b).

Table 2
Aligned sequences among three hydantoinases.

	SGL-1[a] (60–73)	SGL-2[a] (93–100)	SGL-3[a] (150–162)
BstHyd	**H**LD**M**PLGGTVTKD	C**L**TNKGEP	**X**V**F**MA**Y**KNV**F**QAD
BspHyd	**H**LD**M**PFGGTVTAD	C**L**TKKGES	**K**V**F**MA**Y**KNV**F**QAD
BpiHyd	**H**VE**T**VSFNTQSAD	C**Q**QDRGHS	**X**V**F**MA**Y**RGM**N**MID

Sequences in the SGLs are compared among the hydantoinases. The PDB ID of BstHyd, BspHyd and BpiHyd are 1K1D, 1YNY and 1NFG, respectively. Seven residues in the 4 Å vicinity of hydroxide in HPH are marked with bold letters. Residue numbers are referenced on the sequence of 1K1D. X represents carboxylated lysine (Kcx). BpiHyd has some hydrophilic amino acids in the binding site.
[a] Stereochemistry gate loops (SGLs) are structural elements known to play major role in determining the substrate specificity and enantioselectivity in D-hydantoinase [15].

H60 and Kcx150 are involved in metal coordination, and Y155 is catalytically involved via interaction with the hydantoin ring at the transition state [30]. These three residues were conserved among the homologues, and so were excluded from the candidate pool. F152 was also conserved in the aligned sequence and structure (Table 2 and Fig. 2b). L94 was not strictly conserved (BpiHyd has glutamine instead of leucine), but its size is similar among the Hyds. Hydrophobicity and size differences were most significant at the M63 and F159 residues. L94 is critical for the enantioselectivity of Hyd [12]; nonetheless, the present investigation initially focused on the two adjacent amino acid residues. We targeted M63 and F159 as the positions to be redesigned for the improvement of substrate specificity of D-Hyd toward HPH. These positions appeared to modulate the binding capacity of the enzyme while minimally affecting the catalytic machinery.

3.2. Size-based design of a double mutant

It was necessary to decide which amino acid residues to place on the aforementioned design positions to improve substrate specificity. Optimization of the size and hydrophobicity in the positions was the major design goal. Diminishing the size of residue at 159 position progressively increases activity toward HPH [13] because a smaller amino acid enlarges the space available to accommodate the large hydroxyphenyl ring. Since the hydroxyphenyl ring of D-HPH is placed between M63 and F159, we could enlarge the space around the ring by simultaneously changing the size of both amino acids. Considering the previously reported high activity mutant F159A [13], we first designed a mutant designated M63I/F159A, in which residue M63 was substituted by a smaller isoleucine. The designed single/double mutants were found to be stably expressed

Table 3
Catalytic activity of single and double mutation variants.

Position (63/159)	Relative activity[a]
Met/Phe	100
Met/Ser	400 ± 50
Ile/Phe	108 ± 29
Ala/Phe	120 ± 37
Ile/Ser	540 ± 4
Ile/Ala	374 ± 59
Ile/Thr	411 ± 117
Ala/Ser	411 ± 134
Met/Ser	400 ± 50
His/Asn	450 ± 59
Gln/Asn	213 ± 36
His/Arg	168 ± 41
His/Ser	353 ± 62

[a] Activities are expressed as relative values to the value of the wild-type enzyme.

Table 4
Kinetic constants of the wild-type and mutant enzymes.

	Hydantoin			HPH				Fold increase against WT Hyd
	k_{cat} (s^{-1})	K_M (mM)	k_{cat}/K_M ($M^{-1}\,s^{-1}$)	k_{cat} (s^{-1})	K_M (mM)	k_{cat}/K_M ($M^{-1}\,s^{-1}$)		
Wild-type	59 ± 13	78 ± 25	763	18 ± 4	4.9 ± 0.7	3630	4.8	1
M63H/F159N	57 ± 37	416 ± 149	137	62 ± 11	5.1 ± 1.7	12174	89	19
M63I/F159S	8 ± 3	382 ± 212	22	59 ± 13	2.9 ± 1.7	20951	952	198

Values represent the average in duplicate experiments.

using SDS-PAGE analysis (data not shown) and activity toward HPH was elevated 3.7-fold as compared to BstHyd. Because the activity was lower than that of F159A, we tried to complement the optimum space between the two amino acids by increasing the size of residue 159 while M63I was maintained. To accomplish this, F159A was changed to a larger F159S. The resulting M63I/F159S variant displayed 5.4-fold increased activity toward HPH compared to the original BstHyd.

We confirmed the effect of each single mutation in the M63I/F159S mutant by independently measuring the activity of each mutation. The M63I single mutant displayed the same activity as the wild-type enzyme, with the F159S single mutant exhibiting an activity that was elevated 4-fold (Table 3). The smaller sized serine in the design contributed to the increased activity. Further size reduction of the involved amino acid from M63I/F159S to M63I/F159A did not improve the activity (Table 3). Moreover,

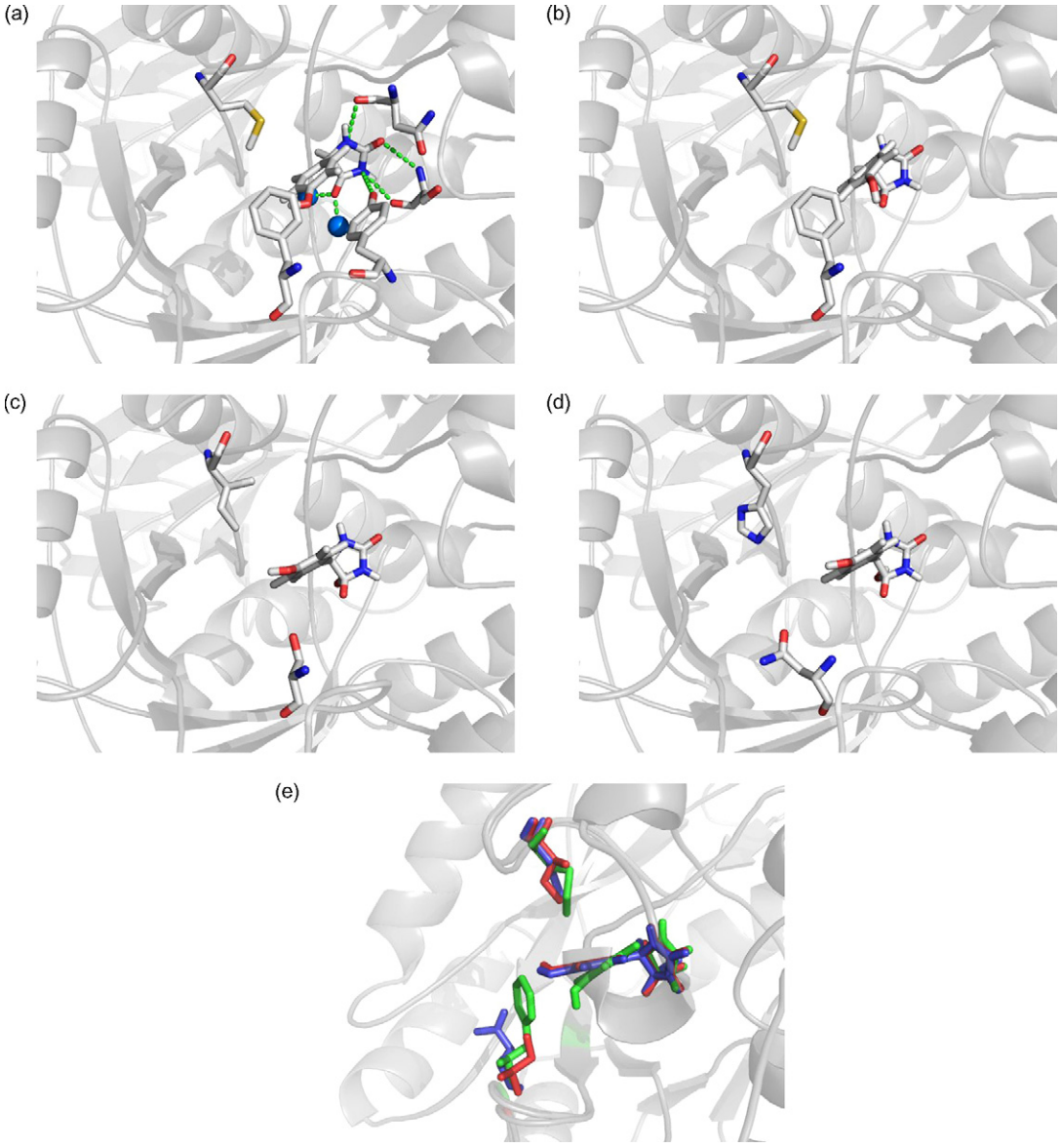

Fig. 3. Docking of hydantoinase with two different states of D-HPH. (a) Ground-state D-HPH with wild-type D-Hyd. Important interactions are indicated with the dotted lines in green. Blue dots are zinc ions. (b–d) Transition-state D-HPH with wild-type D-Hyd (M63/F159), M63I/F159S mutant and M63H/F159N from the same viewpoint. (e) Overlapped docking structure of transition-state D-HPH in a different view. Green: wild-type, red: M63I/F159S, blue: M63H/F159N.

M63I/F159T, which possessed an increased size, also resulted in a decreased activity (Table 3). These observations indicate that 159S has an optimized size with 63I. The M63I mutation also contributed to the size expansion of the binding site (Table 3). The side chain of isoleucine is shorter than methionine, while hydrophobicity is conserved. Although the effect of isoleucine is inherently small, this subtle effect in the M63 mutation proved to be indispensible for the improved activity, along with the F159 mutation. The activities of the F159S single mutant and M63I/F159S double mutant exceeded that of wild-type enzyme by 4-fold and 5.4-fold, respectively.

3.3. Hydrophobicity-based design of a double mutant

High-activity variants were designed by changing the hydrophobicity of the amino acids. The active site residues in Hyd are comprised of hydrophobic amino acids, hence their designation as a hydrophobic pocket. The only exception is the binding pocket of BpiHyd, which has a substrate preference for hydrophilic substituents. BpiHyd has several hydrophilic amino acids such as T62, Q93, and N157 in the substrate-binding site (corresponding residues are numbered 63, 94 and 159, respectively, according to BstHyd numbering in Fig. 2b), which affect the stability and substrate specificity of the enzyme [29]. Considering the size effect, we replaced M63 with histidine, which is similar in size but which possesses a positive charge. F159 was substituted with asparagine, the smallest hydrophilic amino acid. The resulting M63H/F159N variant displayed a 4.5-fold increased activity compared to wild-type BstHyd.

We next sought to optimize the hydrophobicity-designed variant M63H/F159N. As previously noted, the residues around Hyd binding sites consist of hydrophobic amino acids, with the exception of BpiHyd. Similar to BpiHyd, the designed mutant F63H/F159N contained hydrophilic substitutions for the two amino acids. When the Asn was replaced at residue 159 by the similarly sized but hydrophobic Leu, the resulting M63H/F159L mutant displayed an activity only one-third that of M63H/F159N, implying that the hydrophilic residue might interact with the hydroxyl group of the substrate. Replacement of 159N by the larger hydrophilic 159R residue yielded a mutant (M63H/F159R) that also exhibited about one-third the activity of M63H/F159N (Table 3). This result reflects that the 159N mutation affects the activity both with reduced size and with additional hydrophilic interaction. Similarly, the 63H mutation confers both size and charge effects. This is best exemplified by the observation that replacement of 63H by Gln, which is smaller in size and hydrophilic, produced a mutant (M63Q/F159N) that was over 50% less active than M63H/F159N (Table 3). Moreover, the single mutant M63H displayed about 2-fold increased activity compared to the wild-type enzyme.

Although Asn was utilized in the design intended to increase the hydrophilic interaction, the effect of smaller sized Ser was also tested by the creation of mutant M63H/F159S. Although Ser has hydroxyl group, it is known to be marginally hydrophilic according to the hydropathy index [31]. The mutant displayed approximately 20% diminished activity compared to the M63H/F159N mutant (Table 3), which is coincident with the result that an increase in the activity is due to a hydrophilic interaction rather than to a residue size.

To evaluate the alteration in substrate specificity of the designed mutants in more detail, kinetic constants of the best mutants were determined for hydantoin and HPH (Table 4). The M63H/F159N mutant showed a 20-fold increase in substrate specificity compared to the wild-type enzyme. Meanwhile, M63I/F159S exhibited about 200-fold higher specificity for HPH than the wild-type enzyme.

Table 5
Docking scores of the best mutants with D-HPH.

Protein	Ground state Docking energy[a]	Transition state Docking energy[a]	Energy difference G.S. − T.S.[b]
Wild-type	−45.97	−68.99	23.02
M63H/F159N	−49.15	−75.46	26.31
M63I/F159S	−51.40	−77.03	25.63

[a] Lower docking energy indicates more favorable binding.
[b] Docking energy difference is thought to compensate the energy barrier between the high-energy transition-state and ground-state substrate, thus the larger docking energy difference can be an indication of the better enzymatic function.

3.4. Molecular modeling

In the 3D model of the mutants generated by homology modeling, all the amino acid residues had the same coordinate as the template 1K1D, except for several residues around the design positions. Since the binding of D-Hyd to both ground-state D-HPH and high-energy transition-state intermediate D-HPH is important for the enzymatic initiation and activation of the reaction, respectively, binding energy and steric fit in the active site were checked for both ground-state D-HPH and its transition state. As a control receptor for the ligand, we constructed the most plausible docked structures of wild-type 1K1D with both states of D-HPH. The transition state of the D-HPH was modeled as a tetrahedral form at the cleaving carbon atom based on the proposed mechanism of Hyd reaction [32]. Fig. 3a shows the best scored docked structures for 1K1D that exhibited the desirable binding pocket geometry with important interacting molecules (N337, S288, Zn^{2+}, H183, and Y155) in the vicinity of D-HPH. Similarly, the 3D models for the wild-type D-Hyd, M63I/F159S, and M63H/F159N with transition state of D-HPH are shown in Fig. 3b–d, respectively. Higher enzyme activity is usually manifest as a lower binding energy between enzyme and transition-state substrate. Both the M63I/F159S and M63H/F159N mutants were predicted to have lower binding energies with both ground- and transition-state D-HPH compared to wild-type BstHyd (Table 5). In addition, both mutants displayed a larger difference between the binding energies for both states of D-HPH (Table 5, far right-hand column). Since this energy difference is used to overcome the activation energy barrier (the energy difference between ground-state substrate and transition-state substrate), the larger energy difference implies enhanced enzyme activity. The docking simulation also indicated that the wild-type D-Hyd possessed a slightly different docking mode with the transition-state D-HPH from both mutants (Fig. 3e, denoted in green).

We have demonstrated that the substrate specificity of D-Hyd can be rationally designed based on the characteristics of the catalytic site and the target substrate. Rational protein design is based on some particular assumptions about structure–function relationships. Concerning D-Hyd, consideration of the effects of size and charge of important amino acids allowed a more refined design than that was previously obtained [13,33]. The systematic analysis of neighboring mutations provides a more rational design process. In this sense, the CAST method [5] could also be very useful for further improvement. As more protein structures are revealed and experimental data accumulate, rational design including computational design strategies will find more applications.

Acknowledgments

This work was supported by Brain Korea 21 of Ministry of Education, Science and Technology (MEST), Microbial Genomics and Application Center Program of MEST (M105KK000051-06K1101-05110) and Pioneer Research Program for Converging Technology, M10711300001-08M1130-00110 of MEST.

References

[1] Zhao H. Directed evolution of novel protein functions. Biotechnol Bioeng 2007;98:313–7.
[2] Farinas ET, Bulter T, Arnold FH. Directed enzyme evolution. Curr Opin Biotechnol 2001;12:545–51.
[3] Park HS, Nam SH, Lee JK, Yoon CN, Mannervik B, Benkovic SJ, et al. Design and evolution of new catalytic activity with an existing protein scaffold. Science 2006;311:535–8.
[4] Lippow SM, Tidor B. Progress in computational protein design. Curr Opin Biotechnol 2007;18(4):305–11.
[5] Reetz MT, Wang LW, Bocola M. Directed evolution of enantioselective enzymes: iterative cycles of CASTing for probing protein-sequence space. Angew Chem Int Ed 2006;45:1236–41.
[6] Park JH, Kim GH, Kim HS. Production of D-amino acid using whole cells of recombinant *Escherichia coli* with separately and coexpressed D-hydantoinase and *N*-carbamoylase. Biotechnol Prog 2000;16:564–70.
[7] Ogawa J, Shimizu S. Microbial enzymes: new industrial application from traditional screening methods. Trends Biotechnol 1999;17:13–20.
[8] Kim GJ, Park JH, Lee DC, Roh HS, Kim HS. Primary structure, sequence analysis, and expression of the thermostable D-hydantoinase from *Bacillus stearothermophilus* SD1. Mol Gen Genet 1997;255:152–6.
[9] Schulze B, Wubbolts MG. Biocatalysis for industrial production of fine chemicals. Curr Opin Biotechnol 2002;10:609–15.
[10] Chao YP, Fu H, Lo TE, Chen PT, Wang JJ. One-step production of D-*p*-hydroxyphenylglycine by recombinant *Escherichia coli* strains. Biotechnol Prog 1999;15(6):1039–45.
[11] Kim GJ, Lee DE, Kim HS. Construction and evaluation of a novel bifunctional *N*-carbamylase/D-hydantoinase fusion enzyme. Appl Environ Microbiol 2000;66(5):2133–8.
[12] May O, Nguyen PT, Arnold FH. Inverting enantioselectivity by directed evolution of hydantoinase for improved production of L-methionine. Nature Biotechnol 2000;18:317–20.
[13] Cheon YH, Park HS, Kim JH, Kim Y, Kim HS. Manipulation of the active site loops of D-hydantoinase, a $(\beta/\alpha)_8$-barrel protein, for modulation of the substrate specificity. Biochemistry 2004;43(23):7413–20.
[14] Kim GJ, Park JH, Lee DC, Kim HS. Engineering the thermostable D-hydantoinases from two thermophilic *Bacilli* based on their primary structures. Ann N Y Acad Sci 1998;13(864):332–6.
[15] Zhang XY, Niu LX, Shi YW, Yuan JM. The flexibility of the non-conservative region at the C terminus of D-hydantoinase from *Pseudomonas putida* YZ-26 is extremly limited. Appl Biochem Biotechnol 2008;144:237–47.
[16] Cheon YH, Park HS, Lee SC, Lee DE, Kim HS. Crystal structure of D-hydantoinase from *Bacillus stearothermophilus*: insight into the stereochemistry of enantioselectivity. Biochemistry 2002;41:9410–7.
[17] Kim GJ, Lee DE, Kim HS. High-level expression and one-step purification of cyclic amidohydrolase family enzymes. Protein Expr Purif 2001;23:128–33.
[18] Bradford MM. A rapid and sensitive method for quantitation of microgram quantities of protein utilizing the principle of protein-dye-binding. Anal Biochem 1976;72:248–54.
[19] Kim GJ, Kim HS. Optimization of the enzymatic synthesis of *p*-hydroxyphenylglycine from 5-substituted hydantoin using hydantoinase and *N*-carbamoylase. Enzyme Microb Technol 1995;17:63–7.
[20] Takahashi S, Kii Y, Kumagai H, Yamada H. Purification, crystallization and properties of hydantoinase from *Pseudomonas striata*. J Ferment Technol 1978;56:492–8.
[21] Šali A, Blundell TL. Comparative protein modeling by satisfaction of spatial restraints. J Mol Biol 1993;234(3):779–815.
[22] Shen MY, Sali A. Statistical potential for assessment and prediction of protein structures. Protein Sci 2006;15:2507–24.
[23] Brooks B, Bruccoleri R, Olafson B, States D, Swaminathan S, Karplus M. A program for macromolecular energy minimization and dynamics calculations. J Comput Chem 1983;4:187–217.
[24] Vieth M, Hirst JD, Kolinski A, Brooks III CL. Assessing energy functions for flexible docking. J Comput Chem 1998;19:1612–22.
[25] Vieth M, Hirst JD, Kolinski A, Brooks III CL. Assessing search strategies for flexible docking. J Comput Chem 1998;19:1623–31.
[26] Wu G, Robertson DH, Brooks III CL, Vieth M. Analysis of grid-based molecular docking: a case study of CDOCKER – A CHARMM-based MD docking algorithm. J Comput Chem 2003;24:1549–62.
[27] Hermann JC, Marti-Arbona R, Fedorov AA, Fedorov E, Almo SC, Shoichet BK, et al. Structure-based activity prediction for an enzyme of unknown function. Nature 2007;448:775–9.
[28] Radha Kishan KV, Vohra RM, Ganesan K, Agrawal V, Sharma VM, Sharma R. Molecular structure of D-hydantoinase from *Bacillus* sp. AR9: evidence for mercury inhibition. J Mol Biol 2005;347:95–105.
[29] Xu Z, Liu Y, Yang Y, Jiang W, Arnold E, Ding J. Crystal structure of D-hydantoinase from *Burkholderia pickettii* at a resolution of 2.7 Angstroms: insights into the molecular basis of enzyme thermostability. J Bacteriol 2003;185:4038–49.
[30] Abendroth J, Niefind K, Schomburg D. X-ray structure of a dihydropyrimidinase from *Thermus* sp. at 1.3 Å resolution. J Mol Biol 2002;320:143–56.
[31] Kyte J, Doolittle RF. A simple method for displaying the hydropathic character of a protein. J Mol Biol 1982;157(1):105–32.
[32] Thoden JB, Phillips Jr GN, Neal TM, Raushel FM, Holden HM. Molecular structure of dihydroorotase: a paradigm for catalysis through the use of a binuclear metal center. Biochemistry 2001;40:6989–97.
[33] Cheon YH, Park HS, Lee SC, Lee DE, Kim HS. Structure-based mutational analysis of the active site residues of D-hydantoinase. J Mol Catal B: Enzym 2003;26:217–22.